Design of diffractive singlets for monochromatic imaging

Dale A. Buralli and G. Michael Morris

The Seidel aberrations of a rotationally-symmetric diffractive lens with an arbitrary phase profile are presented. It is shown that by a proper choice of phase function and aperture stop position, third-order coma and astigmatism can be eliminated for any chosen conjugate ratio. Since a diffractive lens has an inherent zero value for the Petzval sum, the image plane is flat in both tangential and sagittal meridians. The substrate curvature of the lens may be chosen to introduce a prescribed amount of distortion to allow for use as a Fourier transform lens or a laser scan lens. Examples are given of lens performance in finite conjugate imaging and laser scanning, where the $f-\theta$ condition is satisfied.

I. Introduction

The use of diffractive optical elements can be traced back to Lord Rayleigh, who, in 1871, was apparently the first to make use of the device known today as the Fresnel zone plate.[1] Because of low diffraction efficiency of ~10%, the zone plate has remained mainly an academic curiosity, except for applications in spectral regions where conventional refracting optical materials are not available, such as the soft x-ray region.[2] However, recent developments in the fabrication of high efficiency diffractive optical elements, known as kinoforms,[3] binary optics,[4] or phase Fresnel lenses,[5] have generated a renewed interest in diffractive optics. These fabrication techniques, e.g., precision diamond machining,[6] photolithography,[7] and laser writer systems,[8] provide the designer with the ability to choose a desired diffractive phase function, which may be difficult to obtain using holographic (two-beam interference) techniques.

Since diffractive lenses are essentially gratings with a variable groove spacing, they exhibit an amount of chromatic aberration that is much worse than conventional refractive/reflective optical elements.[9] Thus, the diffractive singlets that we discuss in this paper are limited to monochromatic applications, even though the aberration coefficients we present are valid for all wavelengths and can be used in the analysis of broadband systems which may contain diffractive lenses. Note that diffractive lenses have been used in broadband systems to correct both chromatic and monochromatic aberrations.[10–15]

In this paper we first give a brief derivation of the Seidel aberrations of a diffractive lens. The formulation we present is completely general, allowing for variations in all the design parameters: diffracting zone spacings, bending of the lens substrate, and location of the aperture stop. Then we show how a diffractive singlet can be designed to be coma-free and possess a flat field image for arbitrary imaging conjugates. This design is accomplished by specifying the phase function of the diffractive lens and the location of the aperture stop. The bending of the lens substrate is used to introduce a prescribed (nonzero) amount of spherical aberration or distortion. Control of distortion is useful in the design of lenses for optical processors and laser line scanners, as will be seen in the example designs presented in the paper. After discussing the modeling of diffractive lenses in optical design software, we conclude by providing some design examples, including imaging and lenses for Fourier transformation and laser line scanning ($f-\theta$ lenses).

II. Design of Diffractive Singlets

Throughout this paper we are concerned with rotationally symmetric diffractive lenses which can be described by a phase function of the form

$$\Phi(r) = 2\pi(Ar^2 + Gr^4 + \ldots), \tag{1}$$

where r is the radial coordinate in the diffractive lens tangent plane. Many authors have given the form of the Seidel (third-order) aberration coefficients for diffractive lenses. However, for the purposes of this paper, we need to use the coefficients in their most general form, allowing for variations in substrate curvature

The authors are with University of Rochester, Institute of Optics, Rochester, New York 14627.

Received 6 July 1990.
0003-6935/91/162151-08$05.00/0.

or phase function. Thus, we present a brief derivation here.

Perhaps the simplest way to derive the aberration coefficients is to use the results of Sweatt[16] and Kleinhans,[17] who showed that a diffractive or holographic lens is mathematically equivalent to a thin refractive lens with an infinite refractive index. To third order, the wavefront aberration polynomial W as a function of normalized object coordinate h and normalized polar pupil coordinates ρ and ϕ_p is [18]

$$W(h,\rho,\cos\phi_p) = \tfrac{1}{8}S_{\mathrm{I}}\rho^4 + \tfrac{1}{2}S_{\mathrm{II}}h\rho^3\cos\phi_p + \tfrac{1}{2}S_{\mathrm{III}}h^2\rho^2\cos^2\phi_p + \tfrac{1}{4}(S_{\mathrm{III}} + S_{\mathrm{IV}})h^2\rho^2 + \tfrac{1}{2}S_{\mathrm{V}}h^3\rho\cos\phi_p. \quad (2)$$

In Eq. (2), the Seidel sums S_{I}–S_{V} refer to spherical aberration, coma, astigmatism, Petzval curvature of field, and distortion, respectively. One form of the Seidel sums for a thin lens[19] with aperture stop in contact is conveniently given in terms of dimensionless bending and conjugate parameters E and T, defined as

$$E = \frac{c_1 + c_2}{c_1 - c_2}, \qquad T = \frac{u + u'}{u - u'}. \quad (3)$$

In Eq. (3), c_1 and c_2 are the curvatures of the lens surfaces and u and u' are the angles of the paraxial marginal ray before and after passing through the thin lens. Some of these paraxial quantities are illustrated in Fig. 1. Using these parameters, the Seidel sums for a thin refractive lens take the forms:
spherical aberration,

$$S_{\mathrm{I}} = \frac{y^4\phi^3}{4}\left[\left(\frac{n}{n-1}\right)^2 + \frac{n+2}{n(n-1)^2}E^2 + \frac{4(n+1)}{n(n-1)}ET + \frac{3n+2}{n}T^2\right]; \quad (4a)$$

coma,

$$S_{\mathrm{II}} = \frac{-y^2\phi^2 H}{2}\left[\frac{n+1}{n(n-1)}E + \frac{2n+1}{n}T\right]; \quad (4b)$$

astigmatism,

$$S_{\mathrm{III}} = H^2\phi; \quad (4c)$$

Petzval curvature of field,

$$S_{\mathrm{IV}} = \frac{H^2\phi}{n}; \quad (4d)$$

distortion,

$$S_{\mathrm{V}} = 0. \quad (4e)$$

In Eqs. (4), we have denoted the power of the lens by ϕ (from well-known Fourier optics,[20] the lens power in the pth diffracted order is given by $-2A\lambda p$, where λ is the wavelength of light), the height of the paraxial marginal ray at the lens by y, the Lagrange invariant by H, and the refractive index of the material by n.

To find the aberration coefficients for a diffractive lens, we need to take the limits of the above expressions as $n \to \infty$ and both c_1 and $c_2 \to c_s$, where c_s is the curvature of the diffractive lens substrate. However, we must first rewrite the sums in terms of a different bending parameter, since the parameter E as defined in Eq. (3) becomes indeterminate in the limit as c_1 and c_2 become equal. We shall define a new bending parameter B:

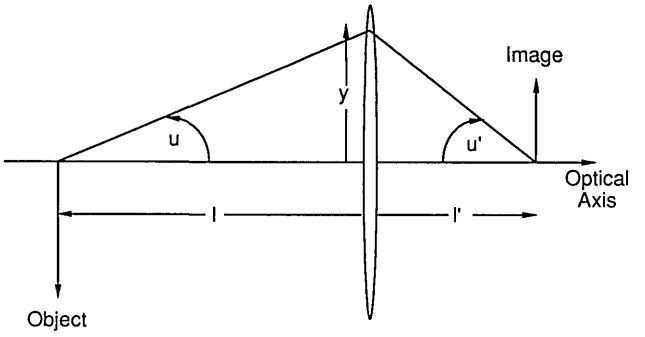

Fig. 1. Illustration of various paraxial quantities. In the figure, l and u' are negative as shown, while the other quantities are positive as shown.

$$B = \frac{c_1 + c_2}{(n-1)(c_1 - c_2)} = \frac{c_1 + c_2}{\phi} = \frac{E}{n-1}. \quad (5)$$

The parameter B is seen to remain finite in the limiting process and be equal to

$$B = \frac{2c_s}{\phi}. \quad (6)$$

With these preliminaries, we can take the limits of the above Eqs. (3) to find the Seidel sums for a diffractive lens. In addition, we need to take account of any asphericity of the lens which can be seen to be equivalent to the effect of the fourth-order term in Eq. (1). With the stop in contact, this term only affects the spherical aberration (in the Seidel terms), so the S_{I} term must be adjusted for the additional optical path length introduced by the fourth-order coefficient G.[21] (It should be noted that we are assuming that the lens is being used in the pth diffracted order. Obvious modifications can be made if other orders need to be considered.) The resulting aberration coefficients for the diffractive lens (stop in contact) are given by
spherical aberration,

$$S_{\mathrm{I}} = \frac{y^4\phi^3}{4}(1 + B^2 + 4BT + 3T^2) - 8\lambda G p y^4; \quad (7a)$$

coma,

$$S_{\mathrm{II}} = \frac{-y^2\phi^2 H}{2}(B + 2T); \quad (7b)$$

astigmatism,

$$S_{\mathrm{III}} = H^2\phi; \quad (7c)$$

Petzval curvature,

$$S_{\mathrm{IV}} = 0; \quad (7d)$$

distortion,

$$S_{\mathrm{V}} = 0. \quad (7e)$$

To allow for the effects of moving the aperture stop to a location distant from the lens, we can use the stop-shift

equations.[22] After the stop shift, the aberration coefficients (denoted by an asterisk) are given by

$$S_{\mathrm{I}}^{*} = S_{\mathrm{I}}, \tag{8a}$$

$$S_{\mathrm{II}}^{*} = S_{\mathrm{II}} + \varepsilon S_{\mathrm{I}}, \tag{8b}$$

$$S_{\mathrm{III}}^{*} = S_{\mathrm{III}} + 2\varepsilon S_{\mathrm{II}} + \varepsilon^2 S_{\mathrm{I}}, \tag{8c}$$

$$S_{\mathrm{IV}}^{*} = S_{\mathrm{IV}}, \tag{8d}$$

$$S_{\mathrm{V}}^{*} = S_{\mathrm{V}} + \varepsilon(3S_{\mathrm{III}} + S_{\mathrm{IV}}) + 3\varepsilon^2 S_{\mathrm{II}} + \varepsilon^3 S_{\mathrm{I}}. \tag{8e}$$

In Eqs. (8), ε is a system-invariant quantity given by

$$\varepsilon = \frac{\delta\bar{y}}{y}, \tag{9}$$

where $\delta\bar{y}$ is the change in paraxial chief ray height (denoted by $\bar{y}$) caused by the stop shift, and y is the height of the paraxial marginal ray at the lens (which is not affected by the stop shift). For the simple system of a singlet, the quantity $\delta\bar{y}$ is just the value of the chief ray height at the lens after the stop shift.

Using Eqs. (7) and (8) we can solve for the stop position (ε) and fourth-order phase term (G) needed to eliminate the Seidel coma and astigmatism for a chosen order p_0 (which will usually be $p_0 = 1$) and chosen wavelength λ_0 by solving the equations $S_{\mathrm{II}}^{*} = 0$ and $S_{\mathrm{III}}^{*} = 0$. The necessary construction parameters are

$$G = \frac{\phi_0^3(1 - T^2)}{32\, p_0\lambda_0}, \tag{10a}$$

$$\varepsilon = \frac{2H}{y^2\phi_0(B + 2T)}. \tag{10b}$$

In Eqs. (10), λ_0 is the design wavelength (i.e., the wavelength at which the lens will be used) and ϕ_0 is the lens power at $\lambda = \lambda_0$, i.e., $\phi_0 = -2\,A\,\lambda_0\,p_0$. [Note that for wavelengths and diffracted orders other than the design wavelength and diffracted order $\phi(\lambda,p) = (p/p_0)(\lambda/\lambda_0)\phi_0$. With these choices of phase function and stop position, the Seidel aberration coefficients for the diffractive singlet in the design wavelength and order are given by

$$S_{\mathrm{I}}^{*} = \frac{y^4\phi_0^3}{4}(B + 2T)^2, \tag{11a}$$

$$S_{\mathrm{II}}^{*} = S_{\mathrm{III}}^{*} = S_{\mathrm{IV}}^{*} = 0, \tag{11b}$$

$$S_{\mathrm{V}}^{*} = \frac{2H^3}{y^2(B + 2T)}. \tag{11c}$$

We see from Eqs. (11) that the third-order aberrations which have the greatest deleterious effect on the off-axis performance of diffractive lenses have been eliminated. Since diffractive lenses have an inherent value of zero for the Petzval sum, elimination of the astigmatism means that the lens has a flat field in both tangential and sagittal azimuths. Aberration coefficients for wavelengths other than the design wavelength λ_0 and other diffracted orders may be found by substituting the construction parameters [Eqs. (10)] into Eqs. (8) using Eqs. (7), although in most situations these diffractive singlets will be limited to monochromatic applications because of the large amount of chromatic aberration inherent to diffractive lenses. Note that we still have the substrate curvature c_s as a free parameter. We may use this parameter to control the remaining spherical aberration or, perhaps more usefully as will be evident in later sections, the distortion.

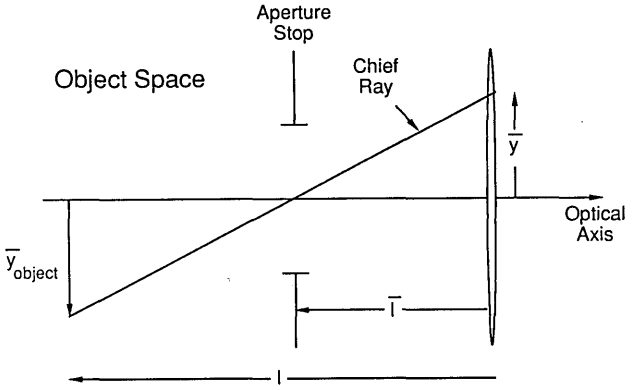

Fig. 2. Construction used to find the position of the entrance pupil.

The substrate curvature and the size of the pupil can be chosen to keep the remaining aberrations within a chosen tolerance. [Unfortunately, neither spherical aberration nor distortion can be made zero, as can be seen from Eqs. (11). For example, a zero value for S_{I}^{*} would imply an infinite value for the stop-shift parameter ε.] The aperture size y can be set by requiring the value of the Strehl intensity to be 0.8 or higher. This implies that, with the choice of best focal plane, a maximum of 0.95 λ_0 of Seidel spherical aberration can be tolerated.[23] This means the aperture size should satisfy

$$y \le \sqrt[4]{\frac{30.4\lambda_0}{\phi_0^3(B + 2T)^2}}. \tag{12}$$

Also, the fractional distortion $(\delta\eta'/\eta')$, conveniently expressed as[24]

$$\frac{\delta\eta'}{\eta'} = \frac{S_{\mathrm{V}}^{*}}{2H} = \frac{H^2}{y^2(B + 2\,T)}, \tag{13}$$

may be controlled by choosing y and B.

It will be convenient for discussion in the examples to follow to convert the expression for stop position, given by the value of ε in Eq. (10b) to explicit expressions for the location of the entrance and exit pupils. For the simple singlet systems discussed in this paper, the aperture stop coincides with the entrance pupil if the stop precedes the lens, and with the exit pupil if the lens precedes the stop. We denote the entrance and exit pupil locations by $\bar{l}$ and $\bar{l}'$, respectively, measured from the lens, with the usual sign convention that a negative value indicates a position to the left of the lens. Referring to Fig. 2, we see that by similar triangles

$$\frac{\bar{y}}{-l} = \frac{\bar{y}_{\mathrm{object}}}{l - \bar{l}}, \tag{14}$$

where l is the distance from the lens to the object and $\bar{y}_{\mathrm{object}}$ is the object height, both negative as shown.

Using Eqs. (14) and (10b), plus the fact that at the object the Lagrange invariant is equal to $H = (u\bar{y})_{\text{object}}$, we can solve for the position of the entrance pupil:

$$l = \frac{2}{\phi_0(B + T - 1)}. \tag{15a}$$

Since the exit pupil is the image of the entrance pupil, the exit pupil location can be found via the imaging equation: $\phi_0 = (1/l') - (1/l)$. The result is

$$l' = \frac{2}{\phi_0(B + T + 1)}. \tag{15b}$$

In the following sections we present some examples of the use of the design equations for imaging and other monochromatic applications.

III. Modeling of Diffractive Lenses

In this section we present a brief description of a technique for modeling diffractive lenses as thin refractive lenses. This approach is necessary if one wishes to use existing optical design software to analyze diffractive lenses, but the optical design program being used does not allow for the evaluation of diffractive or holographic lenses with an arbitrary phase function. As mentioned earlier, a diffractive lens is mathematically equivalent to a thin refractive lens with an infinite index or refraction. Of course, using a value of infinity is not allowable, but a suitably large value of n, say 10,001, will provide adequate accuracy for the vast majority of cases of interest.[25] Once a value for this model lens index, which we shall denote by n_s, is chosen, the curvatures of the model lens must be calculated to give the proper lens power and bending parameter, consistent with Eq. (5). The necessary curvatures are

$$c_1 = \frac{\phi_0}{2}\left(B + \frac{1}{n_s - 1}\right), \tag{16a}$$

$$c_2 = \frac{\phi_0}{2}\left(B - \frac{1}{n_s - 1}\right). \tag{16b}$$

In addition, one of the model lens surfaces must be made aspheric, if the coefficient G in Eq. (1) is nonzero. Since the lens is assumed to have zero thickness, the placement of the asphere on the front or back surface of the lens is immaterial. Assuming a surface sagitta shape of the form

$$z(r) = \frac{cr^2}{1 + \sqrt{1 - (cr)^2}} + dr^4 + \ldots, \tag{17}$$

the necessary aspheric deformation term d is given by

$$d = \frac{\phi_0^3(T^2 - 1)}{32\Delta n}, \tag{18}$$

where $\Delta n = \pm(n_s - 1)$ is the change in refractive index on passing through the aspheric surface of the model lens. (The plus or minus sign for Δn is chosen depending on whether the aspheric surface is on the front or back surface, respectively, of the model lens.) Equation (18) follows from the consideration that an aspheric surface contributes a term of the form $\delta S_I = 8d\Delta n y^4$ to the first Seidel sum[26] and from comparison to the effect of the term Gy^4 in Eqs. (7a) and (10a). If nonmonochromatic performance is to be evaluated, or if the lens is not used with $\lambda = \lambda_0$, the refractive index should be made proportional to wavelength, since the power of a diffractive lens is a linear function of wavelength. Explicitly, the index of the model lens as a function of wavelength and diffracted order is given by

$$n_s(\lambda,p) = \frac{p\lambda}{p_0\lambda_0}[n_s(\lambda_0,p_0) - 1] + 1. \tag{19}$$

Of course, a thin lens produces only a single image, not the multiplicity of images produced by a non-100% efficient diffractive lens. Questions of diffraction efficiency and possible background effects produced by other diffracted orders must be addressed separately from this equivalent lens model. In the evaluation of the sample designs in the following sections, we have used this thin lens model in the design program SUPER-OSLO.[27]

IV. Imaging—Infinite and Finite Conjugates

This example provides a way to demonstrate the use of the design equations presented earlier and of the performance capabilities of diffractive singlets. As will be the case for most practical designs, we choose to use the first diffracted order ($p = p_0 = 1$) and consider only the design wavelength ($\lambda = \lambda_0$). The goals for the design are to correct coma and astigmatism to zero and to keep the absolute value of the distortion to ~1%. The system power is taken to be $\phi_0 = (150\text{ mm})^{-1}$ and the paraxial magnification is $m = -1/3$. Since the magnification is equal to $m = u/u'$, the conjugate parameter for this example is $T = (u + u')/(u - u') = (m + 1)/(m - 1) = -0.5$, and the object and image distances from the lens are $l = -600$ mm and $l' = 200$ mm, respectively. We also choose on object size of $\bar{y}_{\text{object}} = -75$ mm and object space marginal ray angle of $u_{\text{object}} = 1/48 = 0.02083$, which gives a marginal ray height of $y = 12.5$ mm at the lens. This implies a Lagrange invariant of $H = -1.5625$ mm and an image F/No. of $F/8$. If the lens is designed for use at $\lambda_0 = 0.6328\ \mu$m, Eq. (10a) gives a value of $G = 1.0974 \times 10^{-5}\text{ mm}^{-4}$ for the fourth-order phase coefficient, while the r^2 coefficient is $A = -\phi_0/(2\lambda_0) = -5.2676\text{ mm}^{-2}$. If we let $c_s = (-600$

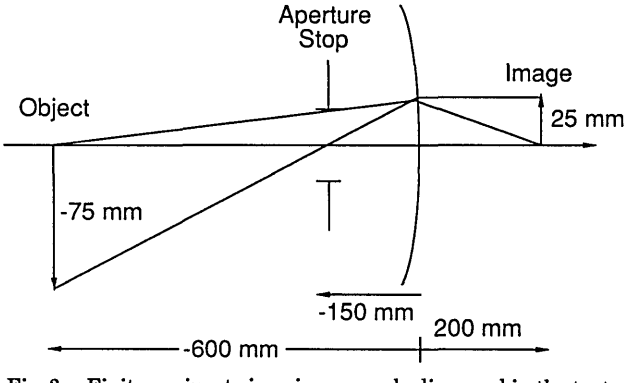

Fig. 3. Finite conjugate imaging example discussed in the text.

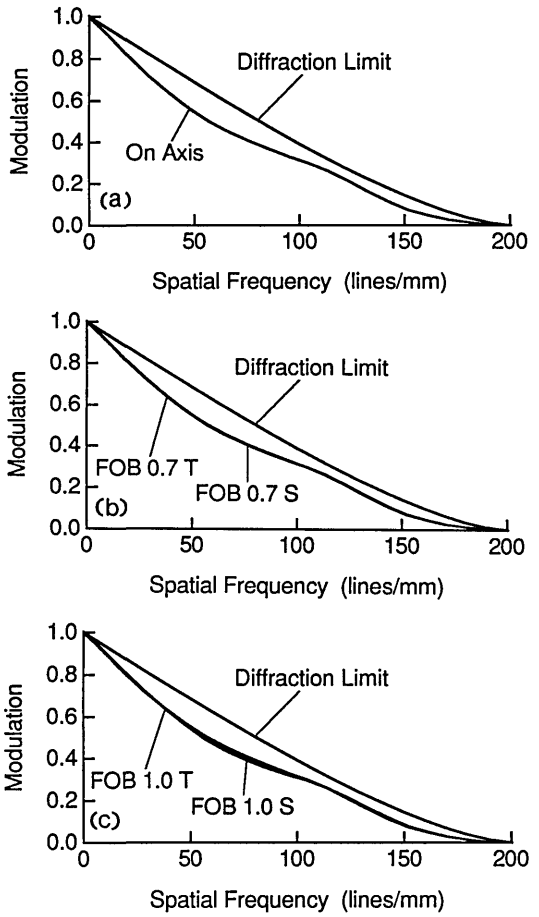

Fig. 4. Modulation transfer functions for a 3:1 imaging lens. The plots are given for three field positions: (a) on-axis, (b) 0.7 field, and (c) full field. In each part of the figure, three curves are drawn: the diffraction limit and lens MTF for tangential (T) and sagittal (S) orientations of the target grating. The S and T curves are formally identical for the on-axis case and nearly indistinguishable in (b) and (c).

mm)$^{-1}$, the bending parameter is $B = -0.5$. The position of the aperture stop, from Eq. (15a), is $\bar{l} = -150$ mm. Equation (13) then gives a fractional distortion of just over -1%, while the remaining spherical aberration is equal to $0.8\lambda_0$. A layout of the system is shown in Fig. 3.

This lens was modeled in SUPER-OSLO as described in the previous section and the resulting MTFs are shown in Fig. 4. The image plane was shifted from the paraxial image plane by an amount which minimized the on-axis rms wavefront aberration (261 μm toward the lens). As can be seen from Fig. 4, the on-axis performance is somewhat reduced from the diffraction limit because of the spherical aberration, but the off-axis performance is essentially the same as the on-axis performance, since the (third-order) coma, astigmatism, and field curvature are all zero. The remaining higher-order aberrations are all much smaller than the uncorrected Seidel spherical aberration. The value of the real ray distortion at the edge of the image is -1.02%, in good agreement with the third-order value given earlier.

V. Fourier Transform Lens

The necessary specifications for a Fourier transform lens can be derived as a special case of the general imaging equations. There is a slight difference in that in this application both the conjugates and the stop position are fixed parameters. Specifically, the lens is designed for infinite conjugates ($T = -1$) and the aperture stop is the front focal plane.[28] When used with collimated illumination, the lens produces the optical Fourier transform in the back focal plane of an object transparency placed in the front focal plane.

Since the conjugate parameter T is equal to -1, Eq. (10a) gives the necessary fourth-order phase coefficient as $G = 0$. Thus, the zone spacings are given by the paraxial approximation to the Fresnel zone formula, i.e., the radius r_m of the mth diffracting zone is given by

$$r_m = \sqrt{2m\lambda_0 f}, \tag{20}$$

where λ_0 is the design wavelength and f is the focal length at the design wavelength. We now need to choose the bending such that the proper aperture stop location is the front focal plane. Substituting $T = -1$ and $\bar{l} = -1/\phi_0$ in Eq. (15a), we find that the necessary bending parameter is $B = 0$, i.e., a planar element.

For a linear relationship between spatial frequency in the object and position in the transform plane, the image height formed by the lens should satisfy the rule $Y = f\sin(\theta)$, rather than the ideal rule of $Y = f\tan(\theta)$, where f is the focal length and θ is the field angle. Thus, the transverse ray error due to distortion should be, to third order,

$$\varepsilon_y = f[\sin(\theta) - \tan(\theta)] = f\left[\frac{\bar{u}h}{\sqrt{1 + (\bar{u}h)^2}} - \bar{u}h\right] = \frac{-1}{2} f\bar{u}^3h^3 + \ldots, \tag{21}$$

where $\bar{u}$ is the paraxial field angle. For the diffractive transform lens described in this section, Eq. (11c) gives the remaining distortion as

$$S_V^* = \bar{u}^3 y. \tag{22}$$

Using the relationship between wavefront error and transverse ray error,[29] i.e.,

$$\varepsilon_y = \frac{1}{n'u'}\frac{\partial W}{\partial \rho_y} \tag{23}$$

and the fact that for an object at infinity $u' = -y/f$, the distortion of the diffractive lens is

$$\varepsilon_{y,\text{diffractive}} = {}^{-1}\!/_2\, f\bar{u}^3h^3 + \ldots, \tag{24}$$

which is the same (to third order) as the desired expression given in Eq. (21). A more detailed analysis of this diffractive landscape lens is given in a recent publication.[30]

VI. Laser Scan Lens

One application in which a prescribed amount of distortion is necessary is that of a lens used for focusing a scanned laser beam onto a flat image field. This lens must satisfy the $f - \theta$ condition, i.e., the image height is

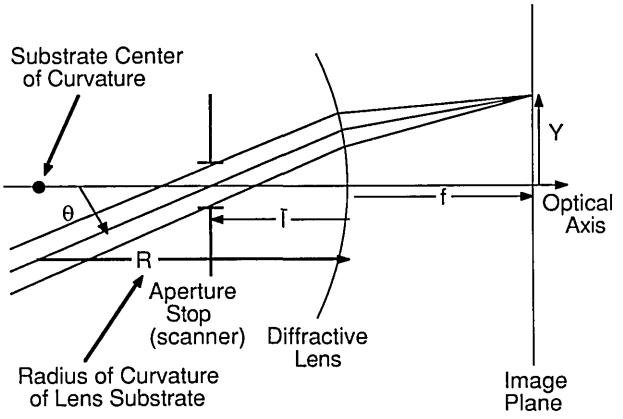

Fig. 5. Layout of the diffractive laser scan lens.

proportional to the input field angle itself, so that the scan velocity across the image plane remains constant. In addition, the focused spot should be formed on a flat field and should remain constant in shape across the image plane.[31] That is, the lens needs to be free from coma, astigmatism, and field curvature, and must have a definite amount of distortion. These are exactly the conditions which a diffractive singlet designed with the equations presented above satisfies.

We assume that the lens is designed to be used with scanned collimated illumination. The location of the aperture stop coincides with the scanner location. As in the case of the Fourier transform lens the conjugate parameter T is equal to -1, so the fourth-order phase coefficient G is equal to zero. We need to find the necessary distortion to satisfy the $f - \theta$ condition. This will determine the bending and, hence, the stop position. To third order, the distortion required is given by

$$\varepsilon_y = f\theta - f\tan(\theta) = f[\tan^{-1}(\bar{u}h) - \bar{u}h] = -\tfrac{1}{3} f\bar{u}^3h^3 + \ldots. \quad (25)$$

Thus, the fifth Seidel sum for a scan lens needs to be

$$S^*_{V,\mathrm{scan}} = \tfrac{2}{3} y\bar{u}^3. \quad (26)$$

Use of this value for the distortion of Eq. (11c) gives the necessary bending as $B_{\mathrm{scan}} = -1$. It then follows that the substrate curvature of the scan lens should be

$$c_{s,\mathrm{scan}} = \frac{-\phi_0}{2}. \quad (27)$$

Also, the entrance pupil position is given by Eq. (15a) as

$$l = \frac{-2}{3\phi_0}. \quad (28)$$

Equations (27) and (28) imply that the substrate has a radius of curvature equal to twice the focal length and is curved toward the stop, which is located a distance equal to $\frac{2}{3}$ the focal length in front of the lens. A diagram of the resulting scan lens system is shown in Fig. 5.

As an example of the performance of this diffractive scan lens, we have evaluated a sample lens with the following parameters:

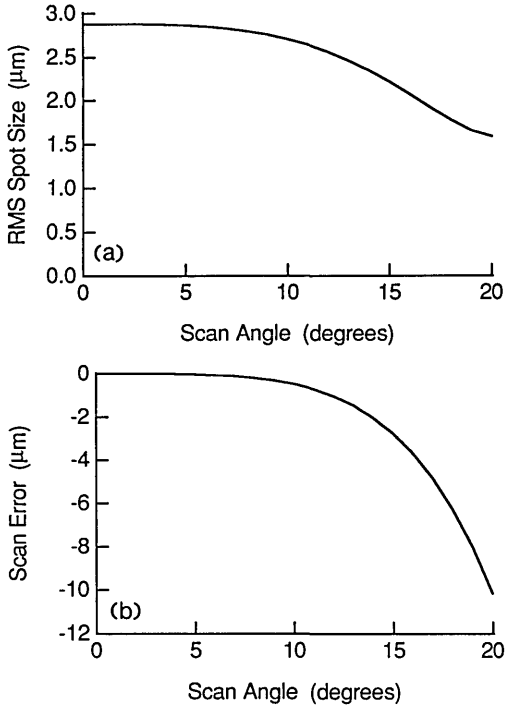

Fig. 6. Evaluation of the diffractive scan lens discussed in the text: (a) geometric rms spot size as a function of scan angle; (b) scan error as a function of scan angle. Scan error is defined as the difference between the centroid of the spot diagram and the product $f \cdot \theta$ for a given angle.

focal length: $f = 325$ mm,
F/No.: $F/20$,
wavelength: $\lambda_0 = 0.6328\ \mu$m,
scan length: ± 4.25 in.,
scan angle: $\theta_{\max} = \pm 20$, and
resolution: ~1600 dots/in.

[We have defined the resolution[32] based on a spot diameter of $d = 1/(2v_{1/2})$, where $v_{1/2}$ is the spatial frequency at which the MTF drops to $\frac{1}{2}$. In this example, $d = 15.7\ \mu$m.] The results of a real ray analysis are shown in Fig. 6. Part (a) shows the geometric spot size as a function of scan angle. Across the field, the geometric spot size is much less than the Airy radius of 15.4 μm, indicating that the diffraction spot size is very close to the diffraction limit. The decrease in spot size with increasing field angle is mainly due to some residual fifth-order Petzval curvature, which has the opposite sign as the uncorrected third-order spherical aberration. Figure 6(b) shows the scan error as a function of field angle. Here, scan error is defined as the difference in image height between the centroid of the spot diagram and the product $f \cdot \theta$ for a given scan angle. We see that as the angle increases, the scan error increases since we have only corrected for the $f - \theta$ condition to third order. However, even at the edge of the scan, the error is only about $\frac{2}{3}$ of a spot diameter.

For scan applications requiring relatively low resolution, one may be able to use a planar scan lens rather than the curved element described above. By giving up the substrate curvature as a design variable, one

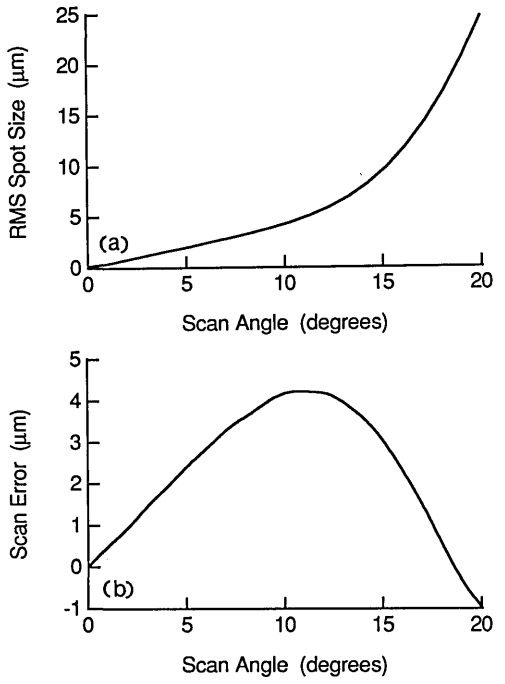

Fig. 7. Evaluation of the planar diffractive scan lens discussed in the text: (a) geometric rms spot size as a function of scan angle; (b) scan error as a function of scan angle.

loses the ability to control the coma. However, the $f-\theta$ condition can still be satisfied and both the tangential and sagittal fields can still be flattened. There are two solutions to $S_{III}^* = 0$ and $S_V^* = (2/3)\, y\bar{u}^3$, with $T = -1$ and $B = 0$. The solutions are (assuming $p = p_0 = 1$) solution A,

$$G_A = \frac{\phi_0^3\left(1-\frac{\sqrt{3}}{2}\right)}{8\lambda_0}, \quad \bar{l}_A = \frac{-1}{\phi_0}\left(1+\frac{\sqrt{3}}{3}\right); \tag{29a}$$

solution B,

$$G_B = \frac{\phi_0^3\left(1+\frac{\sqrt{3}}{2}\right)}{8\lambda_0}, \quad \bar{l}_B = \frac{-1}{\phi_0}\left(1-\frac{\sqrt{3}}{3}\right). \tag{29b}$$

Solution A has a smaller amount of uncorrected coma, but solution B has a smaller scanner-to-lens distance, thus requiring a smaller lens and smaller overall system length. For the more practical case of solution B, the amount of uncorrected Seidel coma is given by

$$S_{II}^* = \frac{-(1+\sqrt{3})}{2}\,\bar{u}y^3\phi_0^2. \tag{30}$$

As an example of the performance of the planar scan lens, Fig. 7 presents an evaluation of the solution B lens for the same parameters as the curved scan lens example presented previously, except that the F/No. is $F/45$, which means that the design resolution is ~700 dots/in. ($d = 35.2\ \mu m$). The increase in spot size with scan angle for small scan angles [see Fig. 7(a)] is caused by the uncorrected coma. For large scan angles, the spot size grows more rapidly with angle. This is primarily caused by fifth-order astigmatism and field curvature. The linear portion of the scan error curve [Fig. 7(b)] is a result of our definition of scan error: coma causes the centroid of the spot to be displaced from the intersection of the chief ray with the image plane.

Although scalar diffraction theory predicts that kinoform lenses should be 100% efficient,[33] results from rigorous electromagnetic grating diffraction theory show that <100% efficiency may be expected from regions of the lens of relatively high periodicity, i.e., where the approximations of scalar diffraction theory are not valid. Light diffracted into orders other than the desired order serves to reduce the image contrast, if this undesired light reaches the image plane. In the case of the scan lens, since most printing systems use a laser power of about twice the threshold exposure power,[34] as long as the diffraction efficiency remains fairly high, say above 70%, the effect of nonunity efficiency will be an effective reduction in system transmittance rather than the writing of unwanted pixels, since the spurious orders contain less than the threshold exposure energy.

VII. Conclusion

For monochromatic applications, diffractive singlets can provide a simple solution to a wide variety of imaging applications, including the laser based systems of Fourier optical processing and laser line scanning. The design equations presented in this paper allow for the production of coma-free, flat field imaging lenses. The wide field performance of these lenses is due in part to the zero value of the Petzval sum for diffractive lenses. This is in sharp contrast to conventional optical systems, in which the Petzval sum is essentially fixed by the first-order layout. With a zero Petzval sum, these diffractive lenses are truly flat field, a key requirement for systems utilizing flat detector arrays or for scanning systems with a flat scan surface.

The authors would like to acknowledge the support of this research by the 3M Company. Dale A. Buralli also acknowledges the support of the Kodak Fellows Program.

Portions of this work were presented as paper MT2 at the 1989 Annual Meeting of the Optical Society of America, held in Orlando, FL, 15–20 Oct. 1989.

References

1. Lord Rayleigh, laboratory notebook, 11 Apr. 1871, quoted in R. W. Wood, *Physical Optics* (Macmillan, New York, 1934), pp. 37–38.
2. J. Kirz, "Phase Zone Plates for X-Rays and the Extreme UV," J. Opt. Soc. Am. **64**, 301–309 (1974).
3. L. B. Lesem, P. M. Hirsch, and J. A. Jordan, Jr., "The Kinoform: a New Wavefront Reconstruction Device," IBM J. Res. Dev. **13**, 150–155 (1969); J. A. Jordan, Jr., P. M. Hirsch, L. B. Lesem, and D. L. Van Rooy, "Kinoform Lenses," Appl. Opt. **9**, 1883–1887 (1970).
4. W. B. Veldkamp, G. J. Swanson, and D. C. Shaver, "High Efficiency binary Lenses," Opt. Commun. **53**, 353–358 (1985); G. J. Swanson and W. B. Veldkamp, "Binary Lenses for Use at 10.6 Micrometers," Opt. Eng. **24**, 791–795 (1985); G. J. Swanson and W. B. Veldkamp, "Diffractive Optical Elements for Use in Infrared Systems," Opt. Eng. **28**, 605–608 (1989).

5. K. Miyamoto, "The Phase Fresnel Lens," J. Opt. Soc. Am. **51,** 17–20 (1961).
6. P. P. Clark and C. Londoño, "Production of Kinoforms by Single Point Diamond Machining," Opt. News **15,** 39–40 (1989); J. A. Futhey, "Diffractive Bifocal Intraocular Lens," Proc. Soc. Photo-Opt. Instrum. Eng. **1052,** 142–149 (1989); G. M. Morris and D. A. Buralli, "Wide Field Diffractive Lenses for Imaging, Scanning, and Fourier Transformation," Opt. News **15,** 41–42 (1989).
7. L. d'Auria, J. P. Huignard, A. M. Roy, and E. Spitz, "Photolithographic Fabrication of Thin Film Lenses," Opt. Commun. **5,** 232–235 (1972).
8. V. P. Koronkevich, "Computer Synthesis of Diffraction Optical Elements," in *Optical Processing and Computing*, H. H. Arsenault, T. Szoplik, and B. Macukow, Eds (Academic, Boston, 1989), pp. 277–313.
9. D. A. Buralli and J. R. Rogers, "Some Fundamental Limitations of Achromatic Holographic Systems," J. Opt. Soc. Am. A **6,** 1863–1868 (1989).
10. A. I. Tudorovskii, "An Objective with a Phase Plate," Opt. Spectrosc. **6,** 126–133 (1959).
11. H. Madjidi-Zolbanine and C. Froehly, "Holographic Correction of Both Chromatic and Spherical Aberrations of Single Glass Lenses," Appl. Opt. **18,** 2385–2393 (1979).
12. G. M. Morris, "Diffraction Theory for an Achromatic Fourier Transformation," Appl. Opt. **20,** 2017–2025 (1981).
13. T. Stone and N. George, "Hybrid Diffractive–Refractive Lenses and Achromats," Appl. Opt. **27,** 2960–2971 (1988).
14. T. A. Fritz and J. A. Cox, "Diffractive Optics for Broadband Infrared Imagers: Design Examples," Proc. Soc. Photo-Opt. Instrum. Eng. **1052,** 25–31 (1989).
15. D. Falkis and G. M. Morris, "Broadband Imaging with Holographic Lenses," Opt. Eng. **28,** 592–598 (1989).
16. W. C. Sweatt, "Describing Holographic Optical Elements as Lenses," J. Opt. Soc. Am. **67,** 803–808 (1977).
17. W. A. Kleinhans, "Aberrations of Curved Zone Plates and Fresnel Lenses," Appl. Opt. **16,** 1701–1704 (1977).
18. W. T. Welford, *Aberrations of Optical Systems* (Hilger, Bristol, 1986), pp. 130–140.
19. Ref. 18, pp. 226–234.
20. J. W. Goodman, *Introduction to Fourier Optics* (McGraw-Hill, New York, 1968), pp. 77–83.
21. Ref. 17, pp. 1702.
22. Ref. 18, pp. 148–152.
23. Ref. 18, pp. 241–246.
24. Ref. 18, p. 146.
25. D. C. Sinclair, "Designing Diffractive Optics using the Sweatt Model," Sinclair Optics Design Notes, Vol. 1, No. 1 (Winter 1990).
26. Ref. 18, pp. 152–153.
27. SUPER-OSLO is a trademark of Sinclair Optics, 6780 Palmyra Rd., Fairport, NY 14450.
28. K. von Bieren, "Lens Design for Optical Fourier Transform Systems," Appl. Opt. **10,** 2739–2742 (1971).
29. Ref. 18, pp. 93–98.
30. D. A. Buralli and G. M. Morris, "Design of a Wide Field Diffractive Landscape Lens," Appl. Opt. **28,** 3950–3959 (1989).
31. R. E. Hopkins and M. J. Buzawa, "Optics for Laser Scanning," Opt. Eng. **15,** 90–94 (1976).
32. See Ref. 31, pp. 93–94.
33. D. A. Buralli, G. M. Morris, and J. R. Rogers, "Optical Performance of Holographic Kinoforms," Appl. Opt. **28,** 976–983 (1989).
34. H. Sonnenberg, "Laser-Scanning Parameters and Latitudes in Laser Xerography," Appl. Opt. **21,** 1745–1751 (1982).